Combined optimisation of design and power management of the hydraulic hybrid propulsion system for the 6 × 6 medium truck

Z. Filipi*, L. Louca*, B. Daran*, C.-C. Lin*, U. Yildir*, B. Wu*, M. Kokkolaras*, D. Assanis*, H. Peng*, P. Papalambros*, J. Stein*, D. Szkubiel† and R. Chapp†

*Automotive Research Center, University of Michigan, Ann Arbor, MI 48109-2121, USA

† National Automotive Center, US Army RDECOM

Abstract: Hybrid propulsion systems are one of the critical technologies on the roadmap to future ultra-efficient trucks. While there is a significant body of work related to hybrid passenger cars and light commercial trucks, there are many open issues related to hybridisation of heavier trucks intended for both on- and off-road use. This work addresses those questions through a systematic analysis of the proposed parallel hydraulic hybrid powertrain for the Family of Medium Tactical Vehicles (FMTV). A representative duty cycle for the FMTV is generated based on information about the typical vehicle mission. A methodology for sequential optimisation of hybrid propulsion and power management systems is applied to a hydraulic hybrid configuration with post-transmission motor location. This analysis is critical in evaluating the fuel economy and mobility potential of the hybrid propulsion system, as well as enhancing our understanding of the phenomena leading to predicted fuel economy values.**Keywords:** heavy vehicles, hybrid propulsion systems, optimisation of propulsion, optimisation of vehicle systems, power management.

Reference to this paper should be made as follows: Filipi, Z., Louca, L., Daran, B., Lin, C-C., Yildir, U., Wu, B., Kokkolaras, M., Assanis, D., Peng, H., Papalambros, P., Stein, J., Szkubiel, D. and Chapp, R. (2004) 'Combined optimisation of design and power management of the hydraulic hybrid propulsion system for the 6 × 6 medium truck', *Int. J of Heavy Vehicle Systems*, Vol. 11, Nos 3/4, pp. 372–402.

1 Introduction

New truck-related research initiatives, such as the 21st Century Truck, Future Tactical Truck Systems and Future Combat Systems, call for significantly improved fuel efficiency, while preserving or improving mobility. For army applications, high operational tempo depends on truck mobility, while improved fuel economy is the key to reducing logistical support. It is estimated that fuel constitutes 70% of the bulk tonnage required to sustain a military force in the battlefield. On the commercial side, trucks account for over 81% of the US's freight business. The total fuel consumption of

commercial trucks is more than 42 billion gallons per year, and in recent years it has been growing at a much faster rate than that of passenger cars. This alarming trend is the result of increased freight volume and commercial truck mileage, as well as an increased number of light trucks due to the popularity of various versions of pick-up trucks and sport utility vehicles. The effectiveness of some of the approaches and technologies for increasing fuel economy, previously developed for passenger cars, is limited when applied to heavier vehicles. Opportunities for mass reduction in trucks are limited due to structural constraints, as well as the fact that the reduction of a truck's weight is typically viewed as one of the avenues for possible increases in payload rating. In addition, medium and heavy trucks are normally equipped with highly-efficient diesel engines, thus limiting opportunities for significant vehicle fuel economy increases through improvements to fuel converter efficiency. Consequently, advanced hybrid propulsion systems are critical enablers on the technology roadmap to future ultra-efficient truck systems.

Vehicle hybridisation generally means using an alternative propulsion component instead of, or in addition to, the conventional engine-transmission-driveline powertrain, as well as adding an energy storage device other than a fuel tank. While this opens up many possibilities related to system architecture, the traditional classification splits hybrids into only two broad categories, series or parallel, depending on whether there is a mechanical connection between the engine and the wheels or not. A variety of propulsion and storage components have been considered, such as electric, hydraulic, pneumatic or mechanical (flywheel). Having an alternative on-board storage device allows for the regeneration and reuse of significant amounts of braking energy, instead of dissipating it as heat. This feature is especially beneficial in truck applications, where there is a lot of braking energy due to the large mass of the vehicles. Consequently, power flows through the hybrid system can be very high, thereby affecting the choice of storage systems. This makes hydraulic propulsion and storage components very attractive for truck applications. Hydraulic pumps and motors are characterised by higher power density than their electric counterparts. In addition, hydraulic accumulators have the ability to accept both high frequencies and high rates of charging and discharging, both of which are not compatible with electro-chemical batteries. However, the relatively low energy density of the hydraulic accumulator requires a carefully designed control strategy for utilising the full potential of the hybrid-hydraulic system's features. In this context, a parallel hybrid architecture is the most attractive and cost-effective option.

While there is a significant body of work related to hybrid passenger cars and small commercial trucks (Aceves and Smith 1995; Belaire, *et al.*, 1997; Duoba, *et al.*, 1996; An and Barth, 1998; Hewko and Weber; and Kosowski and Desai, 2000), as well as specialised vehicles, such as city buses (Marr, *et al.*, 1993; Heidelberg and Reiner, 1989; and Van den Bossche, 1999), there are many open issues related to hybridisation of medium and heavy trucks for both on- and off-road use. Adequate sizing of components, assessment of mobility and handling-related constraints, realistic duty cycles, and strategies for coordinating the primary and assistant power sources, are just a few of the questions that require answers tailored to a specific truck category. Utilising the maximum fuel economy potential of the hybrid propulsion system critically depends on the following: optimal design (size, efficiency characteristics, operating limits, gear ratios in the system, etc.) and component matching; optimal control (power management); and realistic duty cycle for a given vehicle to be used for evaluating its fuel economy. The

difficulty in obtaining a true optimum arises from the complexity of the hybrid system itself, and interdependence of design parameters, control strategies and duty cycles employed. In other words, a power management strategy designed to maximise the fuel economy of a given propulsion system, might be very inappropriate for another system using different components and configurations, e.g. in the case of variations in size, torque and efficiency characteristics or location in the system. A duty cycle emphasising frequent accelerations and decelerations in stop-and-go traffic will lead to a very different optimum configuration and control compared to the one based primarily on highway driving.

Regarding design optimisation, most of the previously published work has focused exclusively on optimal sizing (Triger, *et al.*, 1993; Aceves, *et al.*, 1996; and Moore, 1996). Assanis *et al.* demonstrated the development of a framework for the optimal design of the parallel hybrid-electric system for a mid-size passenger car that links a high fidelity engine model with the overall vehicle system, thus allowing engine design features to be accounted for, in addition to component sizes (Assanis *et al.*, 1999). The development of power management strategies was initially approached by using engineering intuition for devising control rules that would allow load levelling and moving the engine out of the inefficient operating regimes (Hung *et al.*, 2002; Jalil *et al.*, 1997; and Bowles *et al.*, 2000). More recently, fuzzy logic (Won and Langari, 2002) and optimisation algorithms were employed to search for a benchmark to improve rules beyond what engineering intuition can provide (Lin *et al.*, 2001a; Lin *et al.*, 2001b; Lin, *et al.*, 2002; and Wu *et al.*, 2002). However, while design clearly affects optimal power management and vice versa, no attempt has yet been made to address both of them at the same time. The objective of this paper is to develop a methodology for the combined optimisation of design and power management for a hydraulic hybrid system. Such a methodology would allow searching for the absolute optimum and evaluation of the ultimate potential of a certain hybrid technology applied to a vehicle fulfilling a given mission. The particular vehicle selected as the focus of the case study reported here is a member of the Family of Medium Tactical Vehicles (FMTV): a 6 × 6, Class VI truck, capable of carrying a 5 ton payload over smooth or rough terrain.

A predictive system simulation is a pre-requisite for developing a sequential system optimisation methodology. The basis for the FMTV simulation is the high-fidelity Vehicle-Engine SIMulation (VESIM) environment previously developed by Automotive Research Center (ARC) researchers at the University of Michigan (Assanis *et al.*, 2000). VESIM has been validated against measurements for a Class VI truck, and proven to be a very versatile tool for mobility, fuel economy and drivability studies. VESIM emphasised a very high degree of model fidelity, and feed-forward logic, thus enabling studies of transients and easy implementation and evaluation of controllers. Lin *et al.*, (2001a) developed the electric component and power management modules within VESIM to create a hybrid electric propulsion system simulation and used it to conduct an investigation of the optimal control strategy for a medium truck. Expanding this work, Wu *et al.* modelled and integrated the hydraulic components, e.g. axial piston pump/motor and hydraulic accumulator, and addressed the optimal control of an HHV delivery truck (Wu *et al.*, 2002). The hydraulic hybrid FMTV truck is modelled here by adding appropriate components for the 6 × 6 driveline configuration. The prospect of utilising the vehicle system simulation within the optimisation framework, with potentially hundreds or even thousands of executions in a single optimisation run, dictated the application of model reduction techniques and the development of efficient

stand-alone code. Another critical element in the study is the representative duty cycle, generated based on the information about the typical FMTV vehicle mission.

This paper is organised as follows. The methodology for combined design optimisation and power management of the hybrid propulsion system is introduced first. Next, the proposed vehicle architecture, component and sub-system modelling, as well as integration of the complete vehicle system is described. Derivation of the duty cycle is followed by the definition of the optimisation objective, design variables, constraints and optimisation methodology. The first stage of design optimisation is performed, and then the dynamic-programming algorithm is employed to search for optimal trajectories of gear shifting, and engine and motor power commands. The sub-optimal implementable control rules are extracted after studying the main features of the optimal control function. Finally, analysis of results of the final stage of the design optimisation enables evaluation of the hybrid propulsion system fuel economy potential, as well as in-depth understanding of the phenomena leading to specific fuel economy predictions. Conclusions are offered in the final section.

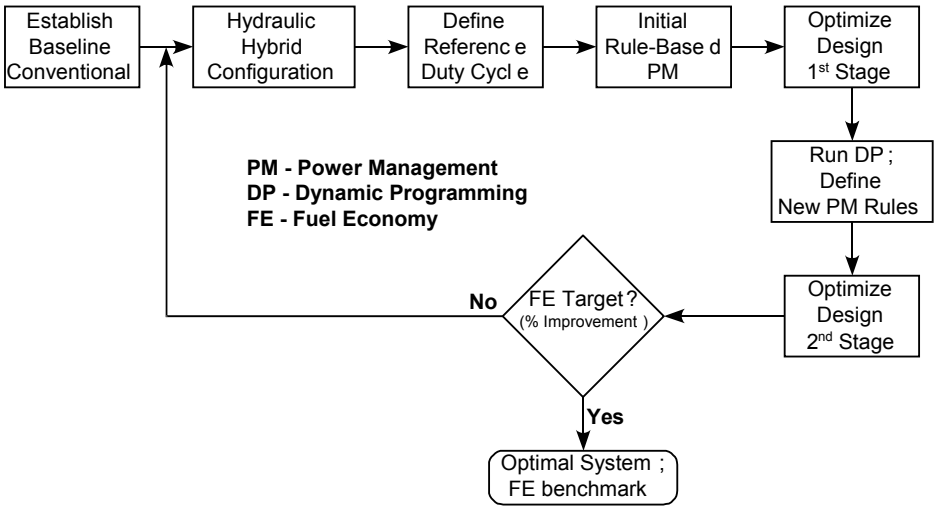

Figure 1 *Methodology for combined optimisation of the design and power management of the hybrid system.*

2 Methodology

This study proposes a sequential approach to optimisation of the parallel hybrid truck propulsion system. The main idea is to first configure the proposed hybrid system, define the design of its main components in the first stage of the design optimisation process, and then optimise the power management strategy for a resulting system configuration. Since modified power management might emphasise different component characteristics, the second stage of the design process allows fine-tuning of the propulsion system design

and evaluation of its true fuel economy potential. Details of the procedure are discussed below.

The methodology relies on the availability of a flexible vehicle system simulation with modules containing predictive models of sub-systems and components. The sequence of critical steps in the process of evaluating the fuel economy potential of the hybrid truck is shown in Figure 1. The development and validation of the vehicle system simulation for a conventional baseline truck is the first step. Then the hydraulic hybrid system simulation is developed based on the proposed system architecture and initial component design. Next, the vehicle mission is analysed and a representative duty cycle is developed. Formulating the initial rule-based power management strategy is the last step before beginning to evaluate the performance and fuel economy of the proposed hybrid configuration. This initiates the first stage in the design optimisation process.

The Sequential Quadratic Programming (SQP) algorithm is selected for solving the design optimisation problem with six design variables. The objective is to maximise fuel economy subject to constraints defined to ensure the ability of the hybrid vehicle configuration to fulfil the same mission as the conventional FMTV truck. A multi-start technique is used to enhance the chances of achieving the true optimum with the derivative-based SQP algorithm. A design of experiments (DOE) technique is applied in order to cover the complete design space efficiently with a relatively small number of starting points.

After determining the optimal (1st stage) values of the design variables, the power management strategy is optimised to extract the most benefit out of the system operating dynamically over a wide range of conditions determined by the driving schedule. The objective is again to maximise fuel economy, and the variables considered are power split in the parallel hybrid system and the transmission shift logic. The approach builds on the success of previous studies pioneering the use of Dynamic Programming (DP) algorithm to search for the optimum control law for a vehicle completing the prescribed driving schedule; (see Lin *et al.*, 2001a; Lin, *et al.*, 2001b; Lin, *et al.*, 2002; and Wu *et al.*, 2002). Using the DP outcome as a benchmark, and analysing simulation results illustrating the behaviour and interactions in the propulsion system, allows extraction of sub-optimal rules that are implementable in a practical controller.

The second stage of the design optimisation process captures the effects of the modified power management on optimum design, and guarantees that the final configuration satisfies prescribed constraints. This sets the stage for the comparison between the conventional vehicle and the one with the optimised hybrid propulsion system, thus allowing assessment of the true fuel economy potential of the selected hybrid concept. In general, if the optimal design does not produce the desired fuel economy improvements, the whole design optimisation procedure can be repeated for a new hybrid configuration, possibly including new component designs, until the fuel economy requirements are met.

3 Modelling the conventional truck system

The vehicle system studied in this work is a 5-ton standard cargo vehicle from the Family of Medium Tactical Vehicles (FMTV) produced by Stewart & Stevenson. It is a 6 × 6, full time all wheel drive truck, with a 7-speed automatic transmission and a gross vehicle

weight of 15 300 kg. The conventional truck is powered by a 6-cylinder, turbocharged, intercooled, direct injection diesel engine with a rated power of 246 kW@2400 rpm. The complete vehicle specifications are summarised in the Appendix.

The schematic of the FMTV three-axle vehicle is given in Figure 2. In the conventional 6 × 6 drivetrain, the engine drives the vehicle through the torque converter (TC), whose output shaft is then coupled to the automatic transmission (Trans). The transmission drives the transfer case (TrC) that equally splits the torque to the front and rear wheels. The front prop-shaft delivers the torque to the front differential (DF). The other output of the transfer case, through the rear-front prop-shaft, delivers power to the rear inter-axle transfer (TrCA) case that further splits the torque to the two rear axles. The first output of the inter-axle transfer case drives the rear-front differential (DR1) and the other the rear-rear differential (DR2) through the rear-rear prop-shaft. Finally, the torque is delivered to the wheels through six half-shafts.

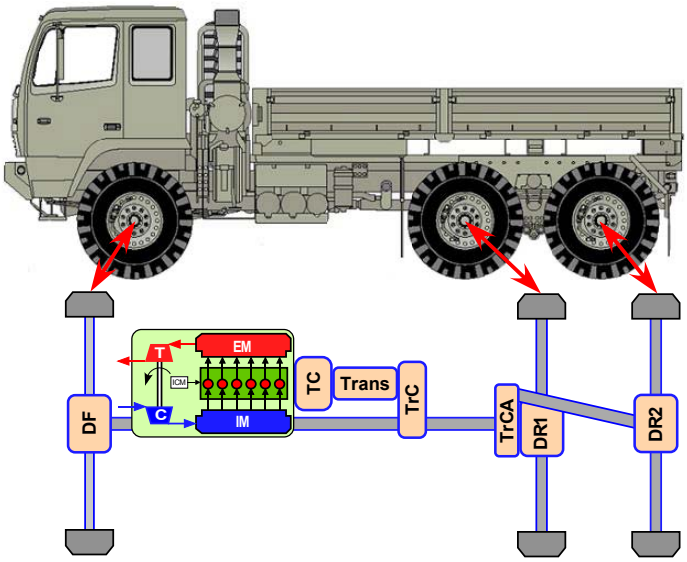

Figure 2 *Schematic of the conventional vehicle propulsion system.*

While high-fidelity models available in the ARC were considered as the starting point (Assanis *et al.*, 2000), the needs of the case study dictated model reduction to a level of fidelity proper for extensive series of calculations within the optimisation framework. The model-reduction procedure ensures preserving features critical to predicting the correct transient behaviour and vehicle fuel economy over a diverse duty schedule (Louca *et al.*, 2003; Louca and Yildir, 2003). The model was developed in the 20SIM modelling environment that supports hierarchical modelling and also allows for physical modelling of sub-systems and components using the bond graph formulation (Karnopp *et al.*, 1990; and Brown, 2001). This modelling environment allows easy modification (addition or removal) of model complexity, as well as automatic generation of the C-code once the simulation is configured; thus facilitating fast execution within the optimisation

framework. The main sub-systems that appear at the top level are the engine, drivetrain, and vehicle dynamics excited by the environment (see Figure 3). One source of excitation is the cyber-driver who provides an accelerator-pedal or braking command based on the current vehicle speed and the desired vehicle speed specified by the duty cycle. The other excitation comes from the road: any unevenness of its profile prescribes a vertical velocity to the tyres at the contact point.

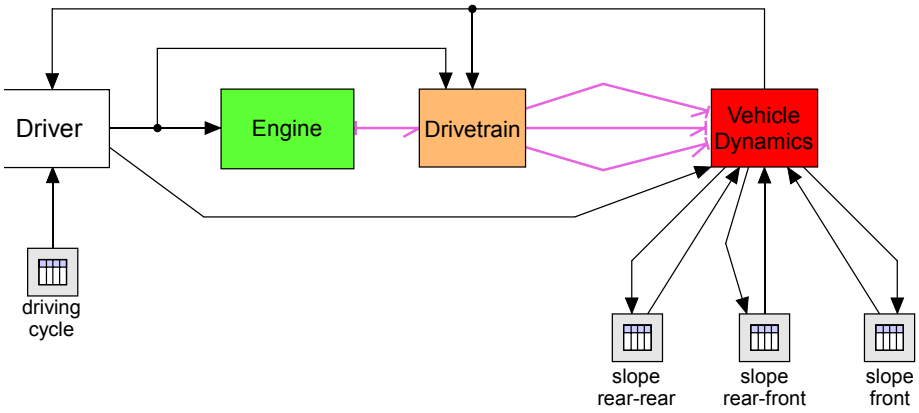

Figure 3 *Conventional FMTV vehicle system modelled in 20SIM.*

3.1 Engine

The engine model used for the conventional 5-ton truck simulation is based on the Caterpillar 3126, an in-line, six cylinder, 7.24 L diesel engine. The specifications of the standard engine are given in the Appendix. The prospect of using the model for optimisation studies, where the vehicle running through a complete driving schedule might be simulated hundreds of times, dictated the modelling approach. Hence, rather than utilising the high-fidelity thermodynamic model previously applied to studies of engine transient response (Assanis *et al.*, 2000; Filipi and Assanis, 2001; and Zhang *et al.*, 1997), a reduced engine model based on the torque look-up table is used here. Figure 4 shows the main components of the engine model configured in 20SIM. The look-up table providing brake torque as a function of instantaneous engine speed and mass of fuel injected is generated from experimental data. The diesel engine fuel injection controller provides the signal for the mass of fuel injected based on driver demand and engine speed. In addition to the base calibration, the controller includes governing functions ensuring stable idle and preventing overspeeding. To retain features of the engine system critical to studies of transient response, a carefully calibrated first-order time lag is introduced in the fuel controller to represent the effect of turbo-lag on transient response during rapid increases of engine 'rack positions', as shown in Figure 4. The instantaneous engine speed is provided as the output of the engine dynamics sub-model, where the rate of change of engine speed depends on the difference between the brake torque and load torque determined by the drivetrain sub-model, and the engine inertia (I:J). A linear torque scaling is added to allow engine variations needed for optimisation

studies. This is deemed appropriate due to the fact that the range of engine scaling will not exceed +/-10%.

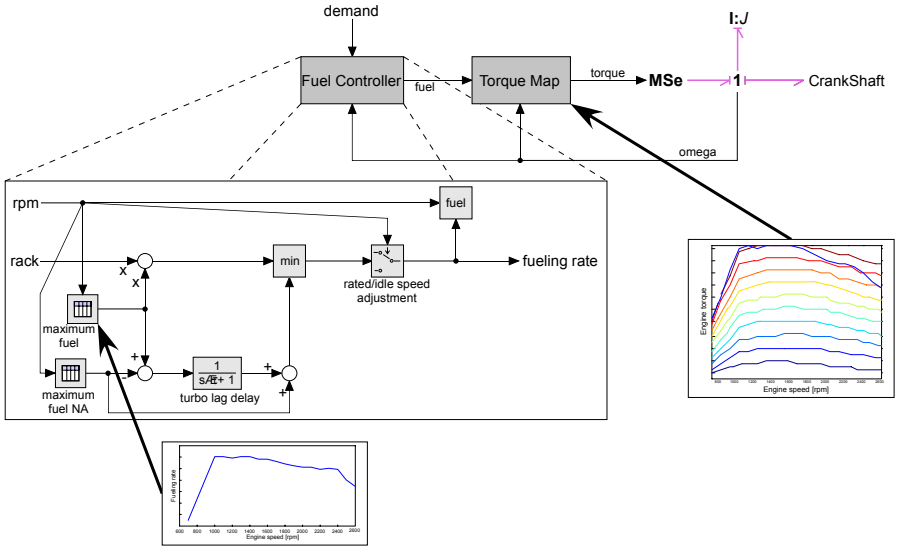

Figure 4 *Diesel engine model in 20SIM consisting of the realistic fuel injection controller, torque look-up table and the engine dynamics.*

3.2 Drivetrain

The drivetrain connects the engine and vehicle dynamics sub-systems. The torque converter input shaft, on one end, and the three drive shafts, on the other end, are the connecting points for the engine and the vehicle dynamics models, respectively (see Figure 5). The inputs are the engine speed and wheel rotational speeds and the outputs are the torques to the wheels and load torque to the engine. Two additional inputs are the driver demand and vehicle speed, which are used by the shift and lock logic to determine the operation of the transmission and torque converter, respectively.

The torque converter is the fluid clutch coupling the engine to the transmission. It has characteristics of a gyrator since the pump and turbine torques are determined by the turbine and pump speeds. The gyrator is a nonlinear and nonpower conserving element that accounts for energy losses due to fluid circulation. The nonlinear modulus of the gyrator is defined by the torque ratio and capacity factor, which are determined as a function of the speed ratio (transmission speed/engine speed). The torque converter includes a lockup clutch that is controlled by a lock logic based on vehicle speed and driver demand. The transmission is modelled as a nonpower conserving transformer that models gear efficiency and different gear ratios for seven gears. The speed reduction in each gear is assumed ideal, while the torque multiplication is reduced by a gear efficiency factor. The transmission fluid churning losses are modelled as a variable nonlinear resistance that varies with the gear number. The differentials and transfer cases are modelled as nonpower conserving transformers with ideal speed reduction but non-

ideal torque multiplication based on a given gear efficiency. Finally the drivetrain inertia and stiffness (equivalent prop-shaft and differential) are included in the model.

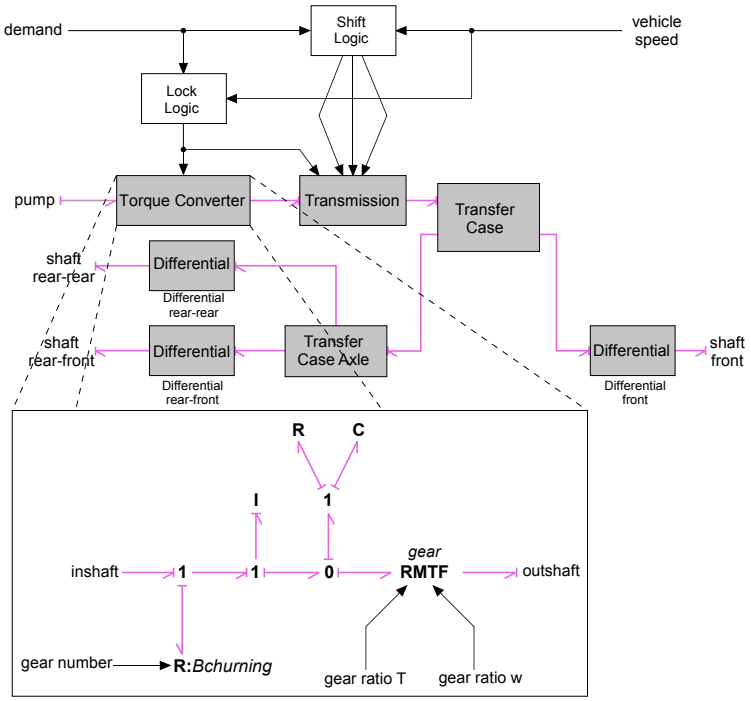

Figure 5 *Drivetrain subsystem.*

3.3 Vehicle dynamics

The vehicle dynamics system considers the wheels, tyres, axles, suspensions, and body of the vehicle. The vehicle is modelled as a collection of rigid bodies that are allowed to move on a plane subject to forces, moments, and rigid constraints. The truck body is modelled as a rigid body that is free to move horizontally and vertically, and to pitch. Three inertial elements (I:Mx, I:My, I:J) are used to represent the dynamics in the three degrees of freedom as shown in Figure 6. The kinematics are described in a body fixed frame (x, y) and represented by the nonlinear Euler equations. Appropriate coordinate transformations are introduced to apply the gravity force which is represented in the inertial frame (X,Y). The body also includes three points for connecting the axles at fixed locations relative to the CG. Finally, aerodynamic drag is modelled by resistive element that is quadratic in the forward vehicle velocity.

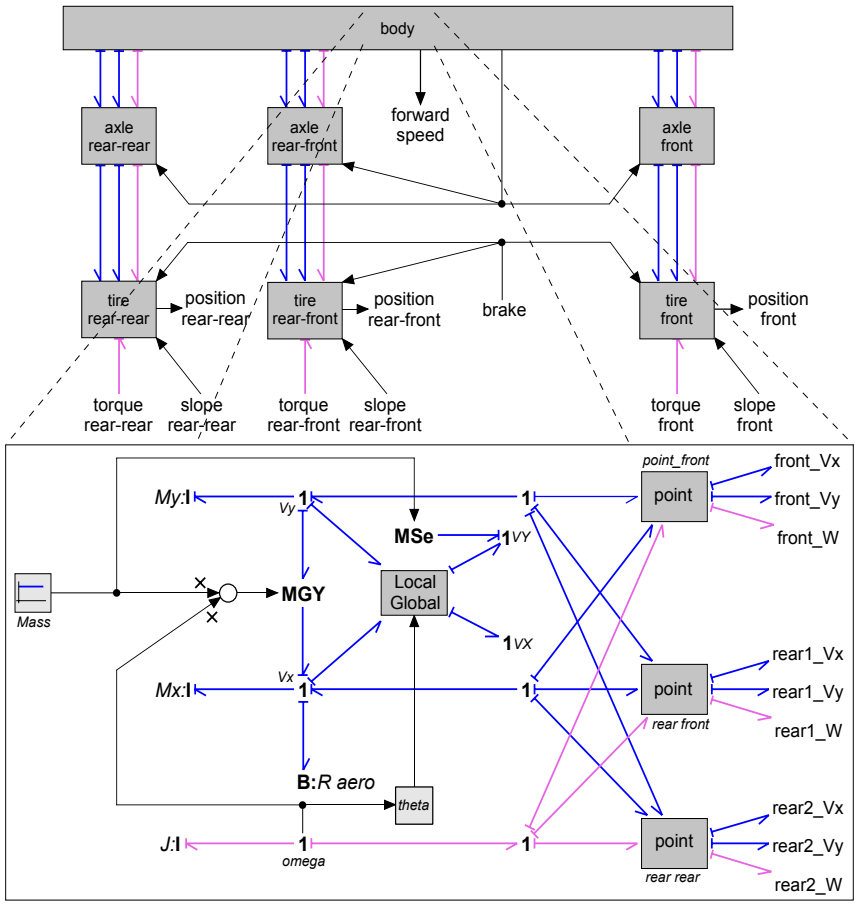

Figure 6 *Vehicle dynamics subsystem.*

Each axle is modelled as a rigid body that is constrained to move on an axis that is perpendicular to the horizontal x-axis of the frame. The axle is also constrained by the suspension, which is modelled as a linear spring and nonlinear shock absorber connected in parallel. The tyre model includes the wheel dynamics and the interaction of the tyre with the road.

Drive torques from the drivetrain are applied at the hub to accelerate the wheel and therefore the vehicle. A simple brake model with viscous and coulomb friction is included to generate the required torque for decelerating the vehicle. The model includes the wheel moment of inertia and bearing viscous losses at the wheel hub, as well as tyre rolling resistance as an additional source of energy loss. Tyre forces in the vertical direction are modelled as a linear spring and damper connected in parallel. The longitudinal traction force is calculated using the Pacejka model taken from (Pacejka and Bakker, 1993). The constants in the Pacejka model are estimated from measured data of the actual tyre.

3.4 Validation

The simulation of the baseline conventional vehicle system has been validated against experimental data provided by the vehicle manufacturer. Measurements were performed during the full-load acceleration test on the proving ground. The comparison of predicted and measured vehicle speed and acceleration profiles shown in Figure 7 indicates excellent agreement, thus validating the overall system simulation.

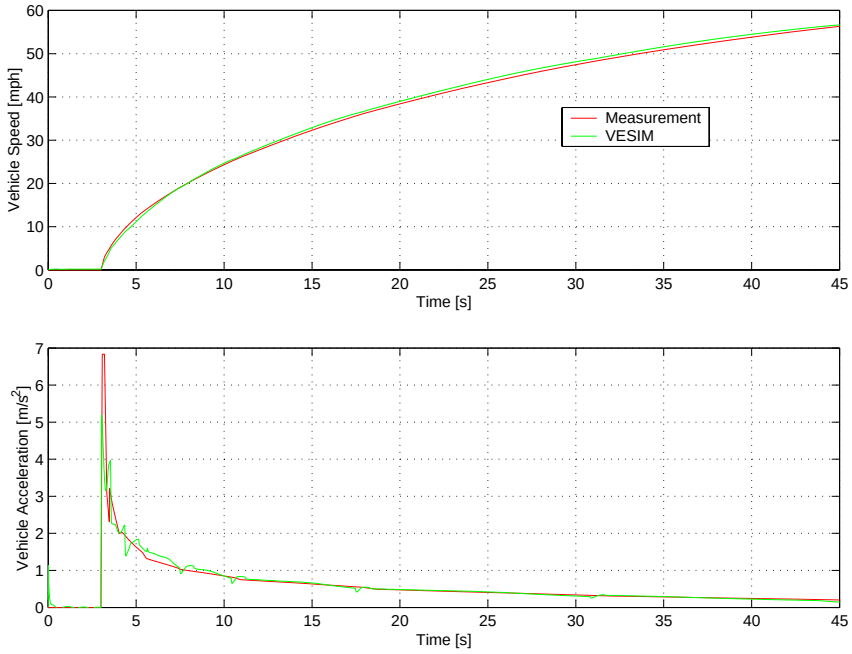

Figure 7 *Speed and acceleration profile comparison.*

4 Hydraulic hybrid vehicle system

The architecture selected for the hybrid hydraulic propulsion system considered in this work is a parallel hybrid with post-transmission motor location. This architecture allows very effective regeneration and re-use of braking energy, while not requiring large energy storage capacity. The variable displacement hydraulic pump/motor (PM) is coupled to the transfer case via a two-speed gearbox, as shown in the schematic in Figure 8. The high gear ratio allows multiplication of pump/motor speed when vehicle speed is slow, thus increasing the power density. When vehicle velocity increases enough to cause the pump/motor speed to reach its limit, the low gear ratio is engaged to prevent over speeding and preserve desirable efficiency. When operating in regenerative mode, the pump absorbs the power from the prop-shaft and transports the fluid from the low-pressure reservoir to the high-pressure accumulator. The energy is stored in the accumulator by compressing the nitrogen gas sealed from the fluid with a piston or a

bladder. Elastomeric foam is added to the gas side to increase the overall heat capacity, and therefore increase the efficiency. When operating in the propulsion mode, the flow is reversed and the pressurised hydraulic fluid drives the motor. The reservoir is constructed in much the same way as the accumulator, but it operates at very low pressures thus merely storing the fluid and has minor contribution to energy flows through the system. Propulsion can be provided by the engine only, motor only or both.

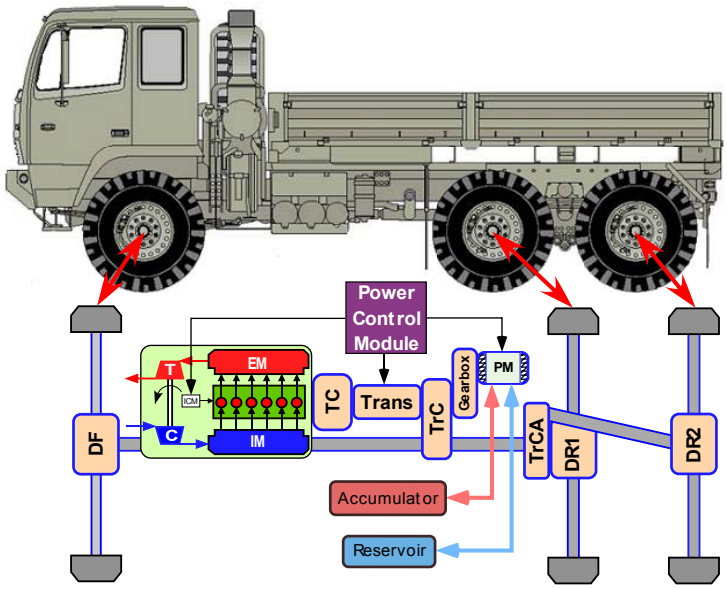

Figure 8 *Schematic of the hybrid hydraulic vehicle system.*

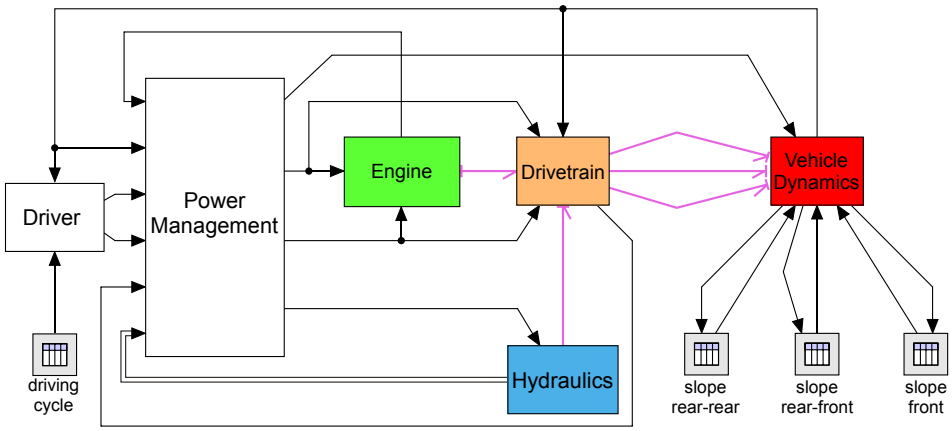

Figure 9 *Hybrid hydraulic vehicle system model in VESIM.*

The hybrid hydraulic vehicle model is an extension of the previously described model for the conventional vehicle. The high-pressure accumulator, the low-pressure reservoir, and the variable displacement pump/motor are connected to define the hydraulic subsystem, which outputs a torque based on the input command. The hydraulic subsystem is integrated with conventional vehicle subsystems, as shown in Figure 9, to produce the hybrid-hydraulic model of the FMTV truck. In addition, a power management module is also included to determine the operating regimes of the engine, transmission, and pump/motor based on the power demand and the available hydraulic fluid in the accumulator – more details about control strategies will be given in the section dedicated to that topic. Details of models for hydraulic components are given in subsequent sub-sections.

4.1 Accumulator model

The accumulator is a high-pressure container whose volume is divided into two parts: one part is designed to hold the hydraulic fluid while the other part contains inert gas such as nitrogen. When the hydraulic fluid is pumped into the accumulator, the sealed gas is compressed and its internal energy increases thus allowing energy to be stored in the accumulator (see Figure 10). The stored energy can subsequently be reused by allowing the hydraulic fluid to flow out of the accumulator and drive the hydraulic motor.

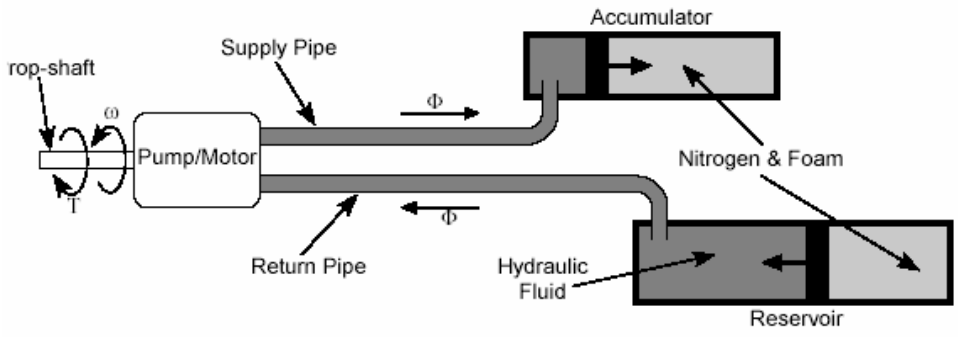

Figure 10 *Hydraulic sub-system configuration.*

The accumulator model captures the gas dynamics (nitrogen) as hydraulic fluid flows in and out of the accumulator causing the compression and expansion of the gas, respectively. For model development, the gas and foam temperatures are assumed uniform. In addition, the gas is assumed real due to the expected high levels of pressure. Given these assumptions, the energy conservation equation, and the real gas law, the following equation is obtained:

$$\frac{dT}{dt} = \frac{1}{m_g c_v + m_f c_f}\left[Q_w - m_g T \left(\frac{\partial p_g}{\partial T} \right)_v \Phi \right] \tag{1}$$

where:

T is the gas and foam temperature

p_g is the gas pressure
m_g is the mass of gas
c_v is the specific heat of gas
m_f is the mass of foam
c_f is the specific heat of foam
Q_w is the heat transfer through the wall
Φ is the fluid flow in the cylinder, equals to rate of change of gas volume (dV/dt)

To complete the description of the gas dynamics, a relationship between the fluid flow (Φ) and the specific volume of gas (v) is introduced, i.e.:

$$\frac{dv}{dt} = \frac{1}{m_g}\Phi \tag{2}$$

For real gas, the Benedict-Webb-Rubin (BWR) state equation is used to correlate the gas pressure, temperature, and specific volume, i.e.:

$$p_g = \frac{RT}{v} + \frac{B_0RT - A_0 - C_0/T^2}{v^2} + \frac{bRT - a}{v^3} + \frac{a\alpha}{v^6} + \frac{c\left(1+\gamma/v^2\right)e^{-\gamma/v^2}}{v^3T^2} \tag{3}$$

The same equation is used to calculate the partial derivative of pressure in Equation (1). The implementation and integration are described in section 4.3.

4.2 Pump/motor model

The hydraulic pump motor is an axial, variable displacement design. The piston travel and displacement are varied by changing the swash plate angle. The modelling approach follows fundamentals analysed by Wilson (1946), and extensions and updates proposed by Pourmovahed *et al.* (1992) and Huhtala (1996). Modelling starts with the equation for the ideal volumetric flow rate through a pump or motor:

$$Q_i = \frac{x \cdot D \cdot \omega}{2\pi} \tag{4}$$

and the ideal torque to operate a pump/motor:

$$T_i = \frac{x \cdot D \cdot \Delta p}{2\pi} \tag{5}$$

where x is the displacement factor that is defined as the ratio of instantaneous displacement to maximum displacement per revolution; D is the maximum displacement per revolution; ω is rotational speed; and Δp is the pressure difference across the pump/motor.

The differences between the real volumetric flow (Q_a) and real torque (T_a) and ideal quantities calculated by Equations (4) and (5) are accounted for by the volumetric and torque efficiencies. The volumetric efficiencies of the pump and the motor are defined by Equations (6) and (7), respectively.

$$\eta_{v,pump} = \frac{Q_a}{Q_i} = 1 - \frac{C_s}{x \cdot S} - \frac{\Delta p}{\beta} - \frac{C_{st}}{x \cdot \sigma} \tag{6}$$

$$\eta_{v,motor} = \frac{Q_i}{Q_a} = \frac{1}{1 + \frac{C_s}{x \cdot S} + \frac{\Delta p}{\beta} + \frac{C_{st}}{x \cdot \sigma}} \tag{7}$$

In the above equations, the terms $C_s / x \cdot S$, $\Delta p / \beta$ and $C_{st} / x \cdot \sigma$ represent volumetric losses due to laminar leakage, fluid compressibility and turbulent leakage, respectively; C_s and C_{st} are coefficients in corresponding terms, and β is the bulk modulus of elasticity of the fluid. The dimensionless numbers $S = \mu\omega / \Delta p$ and $\sigma = \omega \sqrt[3]{D / 2\pi} \Big/ \sqrt{2\Delta p / \rho}$ allow representing all individual terms in a consistent form, where μ and ρ are the viscosity and density of the fluid, respectively.

Similarly, the torque efficiencies are defined as follows:

$$\eta_{t,pump} = \frac{T_i}{T_a} = \frac{1}{1 + \frac{C_v \cdot S}{x} + \frac{C_f}{x} + C_h \cdot x^2 \cdot \sigma^2} \tag{8}$$

$$\eta_{t,motor} = \frac{T_a}{T_i} = 1 - \frac{C_v \cdot S}{x} - \frac{C_f}{x} - C_h \cdot x^2 \cdot \sigma^2 \tag{9}$$

where the terms $C_v \cdot S / x$, C_f / x and $C_h \cdot x^2 \cdot \sigma^2$ represent viscous, mechanical (friction), and hydrodynamic losses. The coefficients in these terms are: C_v for viscous drag, C_f for friction and C_h for hydrodynamic losses.

The model predicts correctly the efficiency trends with respect to changing operating conditions, e.g. speed, pressure, and swash plate angle. This is essential for accurate studies of the system behaviour under transient conditions typically experienced in the vehicle. However, the values of constants need to be calibrated to match the characteristics of a particular design. For the purposes of this study, the model is calibrated to produce relatively high values expected in a pump/motor designed specifically for propulsion.

4.3 Bond graph model

The hydraulic subsystem model implemented using bond graph language (Karnopp *et al.*, 1990; and Brown, 2001) is depicted in Figure 11. The central component is the pump/motor that is modelled with a nonpower conserving modulated transformer (MTF) that accounts for volumetric and torque efficiencies as described in the previous section. For the high-pressure accumulator and low-pressure reservoir the 2-port C element is used, modelling both the fluid and heat transfer dynamics based on Equations (1), (2) and (3). The bond graph language allows the systematic representation of this multi-energy domain component and its interconnection with other components in the subsystem. There are two resistive elements (R_wall_A, R_wall_R) representing the energy exchange of the walls of the accumulator (or reservoir) with the environment (TaA, TaR). In addition, the fluid friction losses in the pipe connecting the pump/motor with the reservoir (and accumulator) are modelled with a nonlinear resistive element (R_pipe_R, R_pipe_A). The State of Charge (SOC) is also calculated since it is needed by the power management module to determine the power split between the diesel engine and the hydraulic motor. The SOC is defined as the ratio of instantaneous volume of

fluid in the accumulator to the total fluid capacity. Finally, the swash plate angle is calculated from the torque command and limits of the pump/motor.

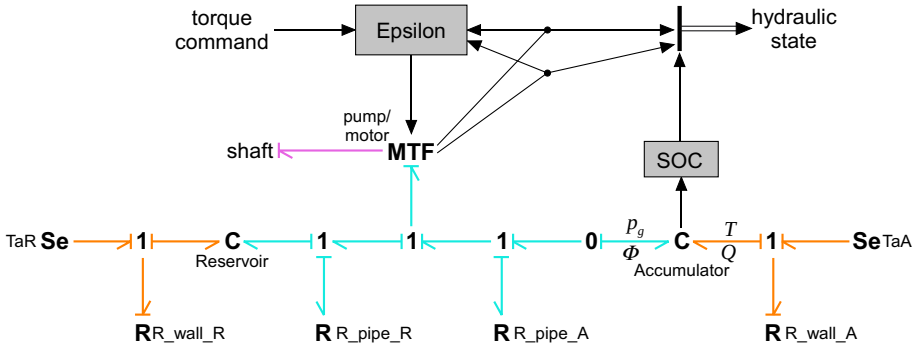

Figure 11 *Hydraulic propulsion subsystem.*

5 Duty cycle

The duty cycle is a critical element in any analysis of fuel economy. Its importance is emphasised in hybrid applications, where complex interactions in the system and the control strategy might play out very differently depending on the driving scenario. While EPA driving schedules are often used for passenger car fuel economy evaluations and specialised cycles have been developed for selected categories of heavier vehicles, e.g. New York City Bus Cycle, or Garbage Truck Cycle, no previous work is available on duty cycles for medium tactical trucks performing tasks both on- and off-road. Therefore, an essential enabler of this study is the development of a custom duty cycle representative of the FMTV's mission.

The FMTV truck's specification provides guidelines in terms of the expected use of the vehicle, i.e. it is anticipated that this 5-ton tactical truck will on average spend 50% of its life span on secondary roads, 20% of the time on primary roads and 30% driving cross country. Primary roads are paved roads with good visibility capable of supporting heavy traffic. Secondary roads have loose and often rough surfaces, and are intended for low density traffic. While highway speeds can be expected on primary roads, it is assumed that secondary roads would be used for delivery of supplies, trips between temporary airstrips and camps or staging grounds, etc. Thus, speed profiles corresponding to secondary roads should have lower peaks and include frequent accelerations and decelerations. The actual profiles are constructed using parts of federal cycles, but eliminating the most aggressive acceleration rates that would not be realistic for medium tactical trucks. For the last segment, the cross-country driving, it is assumed that the driver attempts to maintain a constant speed of 35 mph over the uneven terrain. The elevation corresponds to the parts of the Army test course in Aberdeen, with a peak of roughly 26.5 m, and a maximum span between the peak and the valley of 40 m. The complete driving schedule, comprised of the three segments described above, is shown in

Figure 12. Its duration is 2140 seconds and the total distance is 26.6 km. The predicted fuel economy of the conventional baseline FMTV truck over this duty cycle is 6.27 mpg.

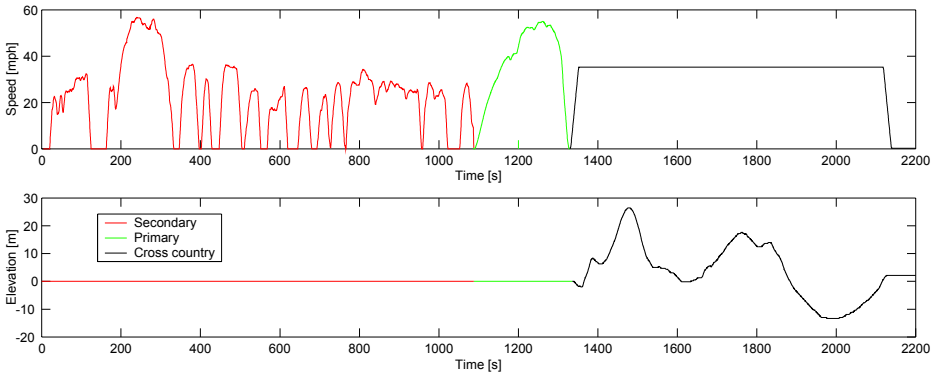

Figure 12 *Duty cycle constructed to represent typical FMTV's mission composed of 50% of driving on secondary roads, 20 % on primary roads and 30 % cross country.*

6 Baseline power management rules

Hybrid Power Management implies devising a control strategy for the most effective coordination between the two power sources, such as the diesel engine and the hydraulic motor, as well as the transmission. The strategy is tailored to a specific goal, which for our purpose is maximising fuel economy. Constraints are imposed to ensure reality, e.g. achieving minimum performance standards and keeping the engine idling when the HHV vehicle is stopped in order to run the accessories, or satisfying special requirements such as driveability or NVH issues. The initial power split rules are adopted from the previous study of optimal control of the Class VI commercial truck performed by Wu *et al.* (2002). These simple rules were developed through analysis of the truly optimal, but non-implementable benchmark, and the use of engineering judgement to capture the main features of the system behaviour. They differ significantly from typical HEV rules (Lin *et al.*, 2001a), in that they emphasise utilisation of high power density of the hydraulic pump/motor for effective regeneration and re-use of braking energy. The accumulator is charged by regenerative braking only. Its state of charge is allowed to fluctuate between nominally empty (SOC = 0) and full (SOC = 1). Braking torque is supplied by the pump and the remaining (if any) is provided by the friction brakes. The engine is not used to charge the accumulator, due to the accumulator's low energy density. In other words, the accumulator could be fully charged at an early stage of the braking event, thus diminishing the regenerative ability of the system. The validity of this approach will be tested after completing the first stage of the design optimisation process. During acceleration, the controller will call upon the motor to satisfy the total power demand whenever there is energy available in the accumulator. If the power requirement is more than what the motor can provide, the engine will supplement the motor power. If the accumulator is empty, the engine becomes the sole power source.

To illustrate this strategy, Figure 13 shows power flows in the system for a simple acceleration/deceleration vehicle schedule. The vehicle is launched using only the motor, thus forcing it to operate at high load (large swash plate angle) resulting in high average efficiency. After about 8 seconds, the motor power becomes insufficient, and the engine is engaged to provide additional power. About ten seconds into the transient, the charge in the accumulator is depleted and the engine becomes the only source of power. When the vehicle speed profile levels off, the engine power drops off to a level sufficient for cruising. Thirty seconds into the transient, a braking signal is sent to the controller and the pump swash plate angle is adjusted to provide the required negative torque. This allows recharging of the accumulator, thus preparing it for the next acceleration. Note that this calculation was performed prior to optimising the design, i.e. the accumulator size is sub-optimal. The original gear shifting logic of the conventional vehicle was used at this stage.

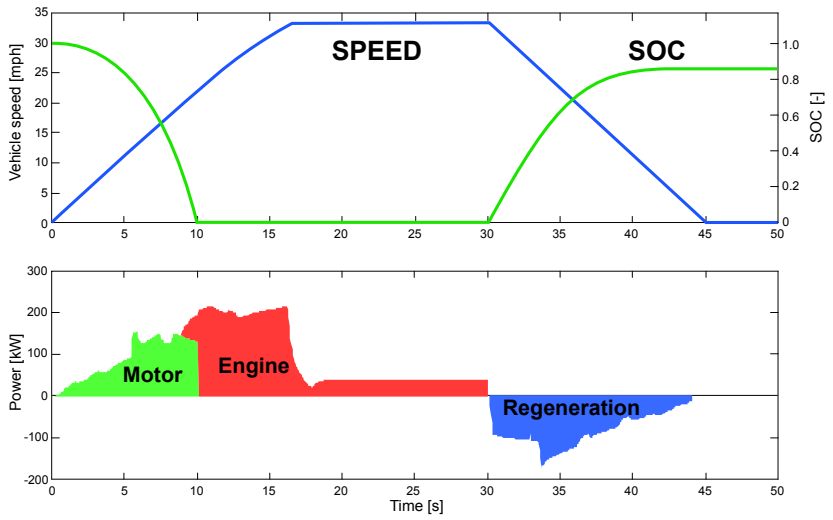

Figure 13 *Power split in the HHV during the simple acceleration/deceleration, determined by the initial power management rules.*

7 Design optimisation – 1st Stage

The complexity of the parallel hybrid propulsion system warrants the use of optimisation routines for determining design parameters of main components and sub-systems leading to the best utilisation of benefits offered by hybridisation. The optimisation problem is formulated as follows:

$$\max_{\mathbf{x}} \quad f(\mathbf{x})$$

$$\text{subject to} \quad \mathbf{g}(\mathbf{x}) \le 0$$

where x are design variables, $f(x)$ is the objective function and $g(x)$ are the constraints. The objective is to maximise fuel economy of the FMTV truck over the representative duty cycle. The design variables and their bounds are summarised in Table 1. The engine size is adjusted by linearly scaling the engine torque and fuel input; thus, the design variable is the engine scaling factor. Linear scaling is deemed appropriate since the range of engine size variation is only +/-10%, the latter being dictated by the aggressive performance constraints discussed in the next paragraph. The hydraulic pump/motor design is defined by the nominal displacement and the high gear ratio between the motor and the propshaft. The low gear ratio is fixed at one in all cases. The accumulator size is based on the volume of fluid that can be stored, but the actual energy content also depends on the corresponding volume and mass of nitrogen gas. The minimum gas volume pertains to the SOC = 1, i.e. accumulator being fully charged. The combination of all three accumulator parameters in turn defines the operating pressure limits, i.e. the precharge pressure and the maximum pressure. Outputs are monitored during all calculations to ensure that they remain within the acceptable range.

Table 1 Design variables and their bounds for the hydraulic hybrid design optimisation.

Design variable	*Range*
Engine size/scale	0.9 -1.1
Hydraulic motor/pump displacement	0.125 - 0.50 litres/rev
Gear ratio between the hydraulic pump/motor and the prop-shaft	1.5 - 3.0
Accumulator size (volume of fluid)	10 - 112.5 litres
Accumulator minimum gas volume	62 - 112.5 litres
Accumulator mass of gas	10.5 - 31.5 kg

The performance constraints that need to be satisfied are derived from the specifications of the conventional vehicle and summarised in Table 2. The 0-45 mph acceleration time constraint is evaluated by assuming that the accumulator State of Charge is at its minimum level (SOC = 0), that is, the accumulator is empty, to ensure maximum rigour and consistency.

Table 2 Performance constraints for design optimisation of the FMTV truck.

Performance attribute	*Constraint*
Gradeability: Continuous vehicle speed on 2% grade	> 55 mph
Gradeability: Continuous vehicle speed on 3% grade	> 45 mph
Acceleration: 0-45 mph	< 24 s

Demanding essentially the same performance from the hybrid truck as from the conventional counterpart distinguishes the study of the tactical trucks from the work focused on passenger cars. Required passenger car performance is typically defined with

some flexibility, specifying the acceptable range rather than demanding exactly the same performance as that of the current production model, and neglecting the indefinitely sustained speed on the grade. Therefore, the nature of the truck's mission leads to relatively more aggressive constraints and that should be taken into account when evaluating final results. The fuel economy will be evaluated over the driving schedule described in section 5, hence, an additional constraint requires that an average driving schedule speed error be less than 1 mph.

The evaluation of the objective and constraints functions requires the execution of the system simulation over the long driving schedule, thus creating the prospect of a very computationally intensive optimisation process. Hence, the highly efficient (Papalambros and Wilde, 2000) general purpose sequential quadratic programming (SQP) algorithm is favoured. Its efficiency comes with a price: since SQP is a gradient-based method, it is prone to being trapped at local optima. Consequently, a multi-start strategy is used to increase the probability of identifying the global optimum.

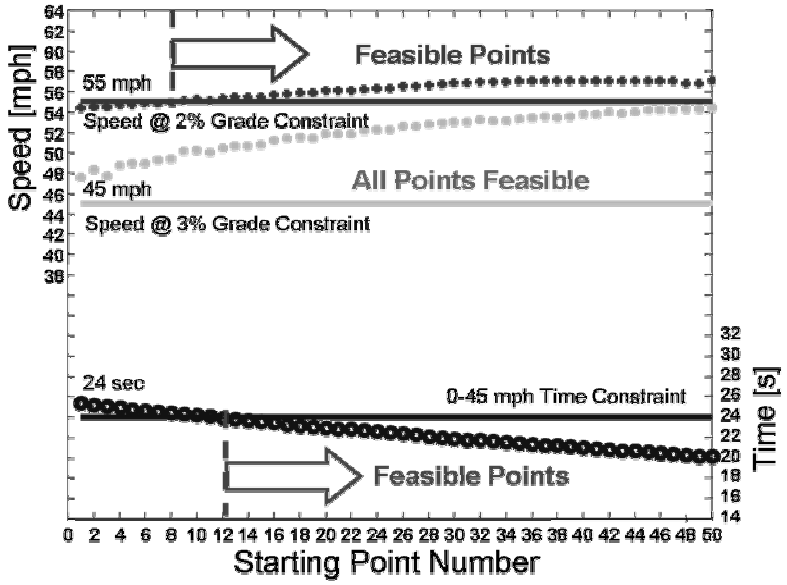

Figure 14 *Evaluating feasibility of points in the Latin hypercube.*

Determining the 'best' starting points is the key part of the multi-start methodology. The design space is defined by the number of design variables (six) and their bounds, shown in Table 1. First, the range of each variable is partitioned into non-overlapping intervals and a value is selected from each interval at random. Covering the complete design space implies combining all the points for the first parameter with all the points for the second etc., leading ultimately to a full factorial combination in the six-dimensional space. In the case of fifty intervals, this would produce more than 15 billion points, a set clearly not feasible for a practical application of multi-starts. Instead, a Design of Experiments (DOE) approach is applied to generate a sample of only 50 points covering the complete six-dimensional space. The Latin hypercube sampling technique (McKay *et al.*, 1979) has been selected to generate the required starting points. Latin

hypercubes produce sets of randomly generated points, hence there is no *a priori* guarantee that any of them provide a good spread over the complete design space. To ensure maximum dispersion, covering the whole design space, a large number of Latin hypercubes is created and tested. The Latin hypercube with the largest *minimum* distance between points is selected (*Maximum Distance Criteria*) (Lunani *et al.*, 1995). The objective and constraints are then evaluated on the DOE points using the vehicle system simulation. The set of feasible points consists of the points that satisfy all constraints. Figure 14 shows that the 0-45 mph acceleration time is the most severe constraint in this application. The continuous speed of 55 mph at the 2% grade requirement is apparently slightly less severe, while all the points easily satisfy the 45 mph at the 3% grade constraint. Finally, the five points with the highest vehicle fuel economy among the feasible points are selected as the best starting points for the SQP optimisation.

The starting points and the initial optimisation results for the hydraulic hybrid truck are given in Table 3. All five runs converge to similar fuel economy numbers, with cases #1, #3 and #5 being slightly better than the other two. The individual design variables also converged to very similar values in these three runs, although the initial points were very different. The fuel economy of 7.6 miles per gallon represents a 21% fuel economy improvement over the baseline conventional truck. The engine scaling is 0.94 in all five cases, and it is determined by the active performance constraint, with the engine being the sole source of power when evaluating all three constraints. The optimiser is obviously finding that engine downsizing is beneficial for fuel economy, and the scaling factor is reduced until one of the performance constraints becomes active – in this case the 0-45 mph acceleration time proved to be critical.

Table 3 Hydraulic hybrid vehicle design: starting values and the corresponding optimum points for the first iteration.

	Engine size/ scale	*P/M gear ratio*	*P/M displ. [l/rev]*	*Acc. min gas volume [l]*	*Acc. mass of gas [kg]*	*Acc. Size [l]*	*F.E [mpg]*
Start #1	0.99	2.69	0.50	104.3	19.9	104.1	7.43
Optimum	0.94	2.12	0.38	105.1	24.7	111.9	7.60
Start #2	0.97	2.72	0.46	99.1	27.2	89.5	7.42
Optimum	0.94	2.08	0.42	97.2	24.3	112.5	7.59
Start #3	0.96	2.45	0.25	106.3	30.2	53.9	7.43
Optimum	0.94	2.12	0.40	103.1	26.0	112.5	7.60
Start #4	0.95	1.59	0.36	68.2	19.1	74.8	7.44
Optimum	0.94	2.47	0.34	87.7	23.6	112.5	7.56
Start #5	0.99	1.53	0.33	74.4	26.8	106.2	7.39
Optimum	0.94	2.05	0.38	112.5	25.2	112.5	7.60

The accumulator size converges to its upper bound of 112.5 L, or very close to it in all runs. The accumulator size in run #1 is 111.9 L, so it can be considered to be at the bound, too. For the three best runs, the pump/motor size, the gear ratio and the accumulator gas-side parameters fluctuate within fairly narrow ranges, indicating

reasonable convergence. As the accumulator size increases, more of the braking energy can be regenerated; therefore the fuel economy increases. However, pressure increases at a faster rate in the smaller accumulator. Increasing the operating pressure increases the amount of stored energy, as well as the pump/motor power density. The best trade-off obviously involves a large accumulator, with the gas-side parameters guaranteeing reasonable average pressure levels. The ratio of gas mass to gas volume, a good indicator of operating pressure levels in the accumulator, varies between 0.22 and 0.25 for the best cases, thus shedding more light on the convergence tendencies. Careful examination of detailed results revealed that the operating pressures in the accumulator never exceeded the pre-set maximum allowable pressure limit of 420 bar. In addition, the power management strategy favouring aggressive launch assist often depletes the accumulator after acceleration events, thus making the accumulator ready for the next regenerative braking.

The pump/motor size is given as the maximum displacement per revolution. As the pump/motor size increases, so does its ability to produce negative torque for braking and positive torque for propelling the vehicle. However, the large motor might be on average less efficient, due to more frequent operation with low swash plate angles, leading to higher relative friction and leakage losses. The optimiser found the best compromise to be around 380 cm^3. The optimal gear ratio results clearly indicate the benefits of speeding-up the pump/motor. Higher speeds mean higher average power levels during both braking and acceleration. In all five cases, the converged value of the gear ratio was above two, despite the fact that the initial values were below 1.6 in two of the cases.

In summary, the results of the first stage in the design optimisation process demonstrate satisfactory convergence that provides good basis for the next stage, i.e. optimisation of power management. Configuration #1 is selected as the optimum, due to the fact that it provides the best fuel economy with the smallest pump/motor and accumulator compared to cases #3 and #5.

8 Optimisation of power management

This section describes the application of an optimisation algorithm for development of a control strategy minimising the fuel consumption of the hydraulic hybrid FMTV. An optimal control problem uses the vehicle configured based on the results of the first optimisation of design (see section 7), and the same combined driving schedule. A Dynamic Programming technique (Bertsekas, 1995) is then utilised to determine the optimal control benchmark. This is followed by the analysis aimed at extracting knowledge about the optimal control and its application to development of the improved rules, though sub-optimal with respect to DP results. The sub-optimal rules are scalable and implementable, and thus suitable for the second and final design stage. Strategies for gear shifting and the distribution of power between the engine and the hydraulic motor are considered. An additional degree of freedom allowed at this stage is the option to charge the accumulator with the engine, rather than only through regenerative braking. This approach is encouraged by the fact that the 1st design stage favoured a large accumulator, thus increasing the chances of possibly finding the charging strategy that would not compromise the regenerative potential.

The control of the HH FMTV is first formulated as an optimal control problem in the DP approach (Lin *et al.*, 2001b; and Lin *et al.*, 2002). The goal is to find the control action of the hybrid powertrain, i.e. the power split between the two power sources and the gear-shifting schedule in the automatic transmission to minimise a cost function, which consists of the total fuel consumption for a given driving cycle, i.e.:

$$J = \sum_{k=0}^{N-1} fuel(k) + \alpha\left(SOC(N) - SOC_f\right)^2$$

where N is the duration of the driving cycle. A terminal constraint on SOC is imposed to maintain the accumulator energy and make it easier to calculate the average fuel economy. SOC_f is the desired SOC at the final time of the cycle.

The DP technique is a powerful algorithm for solving control problems for nonlinear, constrained dynamic systems. DP has the advantage of finding the true optimality within the accuracy of computational grids (Bertsekas, 1995). However, the computational efficiency of DP is low due to the 'curse of dimensionality'. Several techniques, including model reduction, pre-computed look-up tables and vectorised operation, are adopted to accelerate computational speed (Kang *et al.*, 2001; and Lin *et al.*, 2002).

Although the DP approach provides an optimal solution, the resulting control policy is not implementable under real driving conditions because it requires knowledge of the future speed and load profile. The results are, on the other hand, a benchmark against which other control strategies can be compared and learned from. Therefore, the second step in the HHV control development procedure involves knowledge extraction from DP results to obtain implementable rule-based control algorithms. Overall, the behaviours to learn include the transmission gear-shift strategy, the power-split strategy, and the charge-sustaining strategy. Here we assume that the regenerative braking strategy is the same as the initial strategy – use as much regenerative braking as possible, subject to the power limit of the pump and the SOC of the accumulator. The difference between the regenerative braking and the demanded braking power is supplied by the friction brake. This simple regenerative braking strategy assumes that the vehicle handling stability is not an issue – a reasonable assumption given the mass of the vehicle and its 6 × 6 drivetrain.

The gear-shift schedule was found to be crucial for the fuel economy of hybrid vehicles. From the DP results, the gear operational points are plotted on the standard transmission shift-map (see Figure 15). The shift map can be roughly separated into seven regions and the boundary between adjacent regions represents optimal gear shifting thresholds. A new gear-shift map is obtained after a hysteresis function is added to the shifting lines.

There are four possible operating modes of splitting the power demand between the engine and motor when the driver requests a positive power demand: motor-only mode, engine-only mode, power-assist mode (both the engine and motor provide power), and recharge mode (the engine offers additional power to charge the accumulator). Rules for switching between the different modes are established by examining the DP optimisation results. The optimal operating points displaying different operating modes are superimposed on the engine BSFC map given in the engine power vs. speed diagram (see Figure 16). The DP algorithm favours running the engine to charge the accumulator directly when both the total power requirement is small and the accumulator SOC level is low. As a result, the engine's operating points move to more efficient regions at higher

load. The excess energy generated by the engine is absorbed by the hydraulic pump and stored into the accumulator. Directly charging with the engine raises the pressure difference between the accumulator and the reservoir. Consequently, the pump can regenerate more braking energy by producing larger negative torque. On the other hand, if the accumulator SOC level is too high, the accumulator may become full before the end of the braking. In that case, the system would have limited ability to absorb braking energy compared to the baseline power management. Consequently, engine charging needs to be prevented when the SOC level is high.

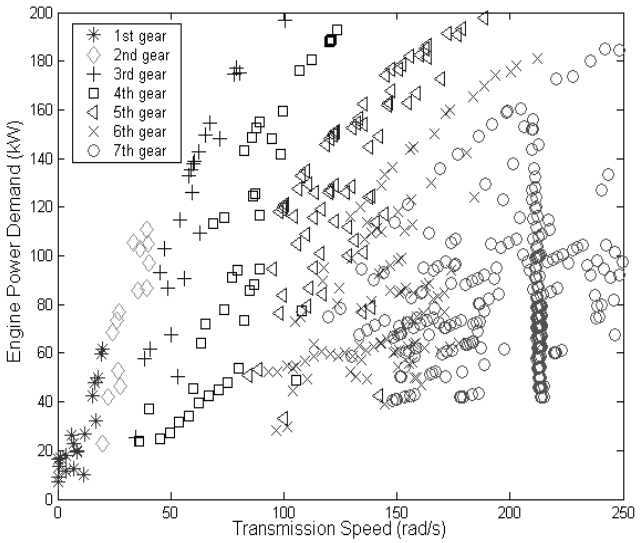

Figure 15 *Optimal gear operation points.*

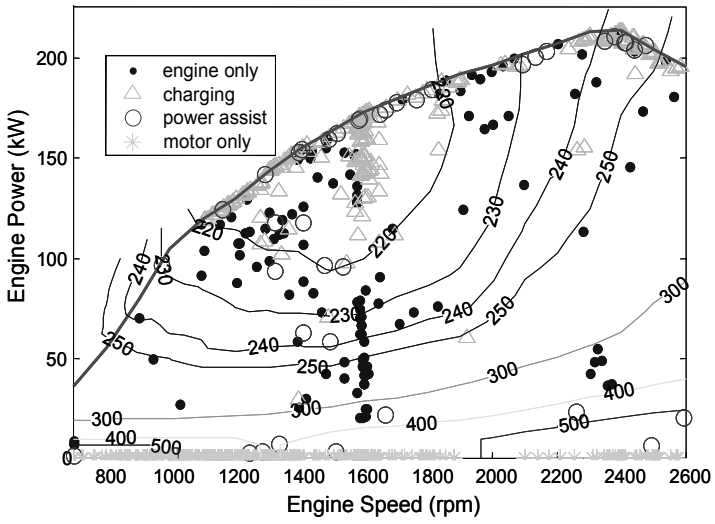

Figure 16 *Optimal operating modes from dynamic programming for the hybrid hydraulic configuration.*

Based on the above observations, a set of new rules are developed to govern direct charging of the accumulator by the engine. There are two limits on the accumulator SOC level. When the SOC is above the high limit of 0.5, engine direct charging is not allowed, hence maintaining enough accumulator capacity for the next regeneration event. When the SOC is below the low limit of 0.3, engine direct charging is allowed. Between these two limits, direct charging may or may not be allowed depending on the vehicle speed: when the vehicle speed is low, that is less than 10 mph, direct charging is allowed; otherwise, direct charging is not allowed. The reason to consider the vehicle speed as the criterion is based on the following: low vehicle speed means less kinetic energy and less space requirement when braking happens. When direct charging is not allowed, rules similar to old rules are used to split the total power requirement between the engine and the motor. In case direct charging is allowed, the engine produces as much power as possible to satisfy the propulsion power requirement and to simultaneously charge the accumulator through the hydraulic pump. In summary, the new strategy attempts to push both the hydraulic pump/motor and the engine into the high load/high efficiency operating regions.

The optimal benchmark control law applied to the HH FMTV truck driving through the complete duty cycle increases fuel economy to 9.06 miles per gallon. However, after the new sub-optimal, but implementable rules are developed and applied, the practically achievable fuel economy is determined to be 8.34, a 34% improvement over the conventional baseline. From the perspective of practical use, the new rules are raising the issue of controlling the highly dynamic processes. The current control strategy leads to frequent switching between the engine's normal operation and the accumulator charging mode, which could create peak acceleration and jerk at the seat unacceptable in terms of driver feel. Additional control functions would have to modulate the step-in and step-out of the engine torque during charging in order to establish a process transparent to the driver. While this certainly poses a challenge, the analogy with controlling the diesel engine during recharging of the Lean-NOx trap indicates that the challenge can be addressed using the latest advances in engine/driveline control technologies.

9 Design optimisation – 2nd stage

Application of the new power management rules motivates the second design optimisation stage for two reasons. Firstly, the system behaves very differently with the new rules, and it is reasonable to assume that it might require different matching of components and design parameters. Secondly, the development of the optimal control does not include evaluation of the performance constraints, hence the second stage of the design optimisation will automatically guarantee that the constraints are satisfied. The same methodology with multi-start SQP optimisation is followed as in the first design optimisation stage. The best initial and final optimised design configurations are compared in Table 4.

The engine size in the hybrid hydraulic configuration increases in the second stage due to changes in the power management algorithm. Since the new rules allow the accumulator to be recharged by the engine, the average engine power requirement is increased and the engine size is no longer determined by the 0-45 mph acceleration

constraint. In addition, the increased engine size partly compensates for the effects of a new gear shifting logic and prevents any significant deterioration of vehicle performance.

Table 4 Hybrid-hydraulic vehicle configurations resulting from the initial and final optimisation of design.

Optimum	*Eng. size/ scale*	*P/M gear ratio*	*P/M disp. [l/rev]*	*Acc. min gas volume [l]*	*Acc. mass of gas [kg]*	*Acc. size [l]*	*F.E [mpg]*
1st Stage.	0.94	2.12	0.38	105.1	24.7	111.9	7.6
2nd Stage.	1.01	2.5	0.36	70.0	15.5	109	8.3

The pump/motor gear ratio and the P/M maximum displacement are also affected by the new rules. A greater P/M gear ratio and a smaller P/M maximum displacement are preferred by the optimiser. This combination actually preserves the power density of the pump/motor, while moving the motor operating conditions toward higher loads at very low speeds. The accumulator size is still very close to the upper bound, but the gas-side parameters and the engine charging strategy lead to higher average accumulator pressures. Thus, a smaller hydraulic pump can produce power levels equivalent or higher then those observed with the larger pump in the 1st design stage. The maximum accumulator pressure constraint has been made slightly more stringent, preventing the pressure to exceed 350 bar. The comparison between results obtained for all five starts of the SQP optimisation indicates less convergence after the second design stage than after the first. It seems that the new control strategy makes the system response surface rougher, thus increasing the danger of the optimiser terminating at a local minimum. Given the complexity of the overall problem of defining the most efficient, yet practical propulsion system configuration, it is not surprising that the absolute optimum is not necessarily obvious. However, the fact that analysis of results clearly points to the most desirable solution, as well as the high consistency among the predicted maximum fuel economy levels, confirm that the proposed methodology represents a very valuable decision-making tool.

The predicted fuel economy of the final configuration of the hybrid hydraulic vehicle with improved power management is 8.3 mpg. This represents a 32% improvement over the conventional vehicle. Even though a number of hydraulic propulsion system parameters have changed, the final amount of regenerated energy calculated over the duty cycle does not change significantly between the first and second design stages. To highlight associated mobility issues, the longitudinal acceleration test results for the conventional and hybrid hydraulic configurations are illustrated in Figure 17. When starting with the full accumulator, the hydraulic hybrid propulsion significantly improves the ‘dash speed’, i.e. reduces the 0-25 mph and 0-45 mph times.

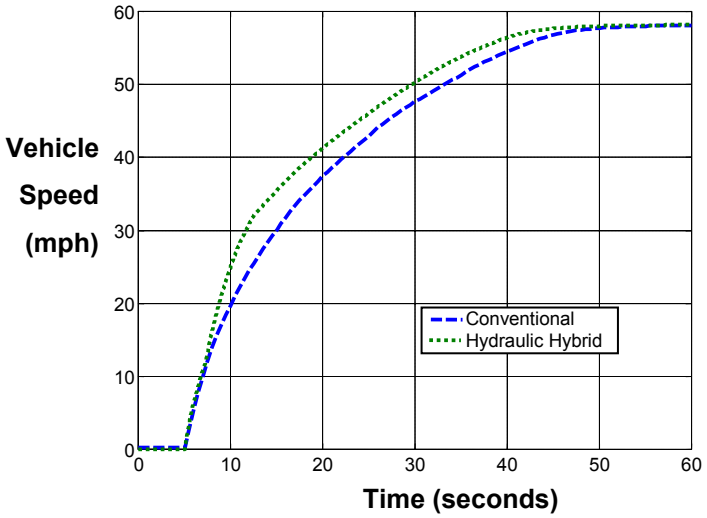

Figure 17 *Comparison of the speed profiles during the full load FMTV acceleration: conventional vs. hydraulic hybrid propulsion (initial SOC=100%).*

10 Conclusions

The effectiveness of the proposed methodology for combined, sequential optimisation of design and power management of the hydraulic hybrid propulsion system is demonstrated through the study of the hydraulic hybrid propulsion system for the 6 × 6, 5 ton, medium tactical truck. Critical enablers of the case study are:

- the development of a predictive, reconfigurable HHV vehicle system simulation;
- the development of a design optimisation framework and its application under real-life constraints;
- the development of a realistic duty cycle derived from the planned vehicle mission;
- and the establishment of a methodology for improving power management rules based on the optimal benchmark derived from application of Dynamic Programming.

The combined optimisation approach revealed the potential for improving the fuel economy of the medium tactical truck (FMTV) by 32% through application of the hydraulic hybrid propulsion technology. Roughly two-thirds of the improvement was achieved through optimisation of design, while the remaining one third can be attributed to the new power management strategy.

Acknowledgements

The authors would like to acknowledge the technical and financial support of the Automotive Research Center (ARC) by the National Automotive Center (NAC) located within the US Army Tank-Automotive Research, Development and Engineering Center (TARDEC). The ARC is a US Army Center of Excellence for Automotive Research at the University of Michigan, currently in partnership with University of Alaska-Fairbanks, Clemson University, University of Iowa, Oakland University, University of Tennessee, Wayne State University, and University of Wisconsin-Madison. In particular, Jim Yakel provided technical guidance related to the FMTV Program strategic objectives. Additionally, Walter Budd and David Perry of Stewart & Stevenson are recognised for providing critical information and data for the FMTV tactical truck.

References

Aceves, S.M. and Smith, J.R. (1995) 'A hybrid vehicle evaluation code and its application to vehicle design', SAE paper 950491, Warrendale, PA.

Aceves, S.M, Smith, J.R., Perkins, L.J., Haney, S.W. and Flowers, D. (1996) 'Optimization of a CNG series hybrid concept vehicle', SAE paper 960234, Warrendale, PA.

An, F. and Barth, M. (1998) 'Critical issues in quantifying hybrid electric vehicle emissions and fuel consumption', SAE paper 981902, Warrendale, PA.

Assanis, D., Delagrammatikas, G., Fellini, R., Filipi, Z., Liedtke, J., Michelena, N., Papalambros, P., Reyes, D., Rosenbaum, D., Sales, A. and Sasena, M. (1999) 'An optimization approach to hybrid electric propulsion system design', *Mechanics of Structures and Machines*, Volume 27, No. 4, pp. 393-421.

Assanis, D.N., Filipi Z.S., Gravante S., Grohnke D., Gui X.,Louca L.S., Rideout G.D., Stein J.L. and Wang Y. (2000) 'Validation and use of SIMULINK integrated, high fidelity, engine-in-vehicle simulation of the international class VI truck', SAE Paper 2000-01-0288, Warrendale, PA.

Belaire, R.C., Lawrie, R.E. and Skellenger, G. (1997) 'Energy converter for the PNGV vehicle', SAE paper 972677, Warrendale, PA.

Bertsekas, D.P. (1995) *Dynamic Programming and Optimal Control*, Athena Scientific.

Bowles, P., Peng, H. and Zhang, X. (2000) 'Energy management in a parallel hybrid electric vehicle with a continuously variable transmission', *Proceedings of the American Control Conference*, Vol. 1, pp. 55-59, IEEE, Piscataway, NJ, 00CB36334.

Brown, F.T. (2001) *Engineering System Dynamics: A Unified Graph-Centered Approach*, Marcel Dekker, ISBN 0-8247-0616-1, New York, NY.

Duoba, M., Larsen, R. and LeBlanc, N. (1996) 'Design diversity of HEVs with example vehicles from HEV competitions', SAE Paper 960736, Warrendale, PA.

Filipi, Z.S. and Assanis, D.N. (2001) 'A non-linear, transient, single-cylinder diesel engine simulation for predictions of instantaneous engine speed and torque', *ASME Journal of Engineering for Gas Turbines and Power*, October, Vol. 123, No. 4, pp. 951-959.

Heidelberg, G. and Reiner, G. (1989) 'Magnetodynamic Storage Unit - test results of an electrical flywheel storage system in a local public transport bus with a diesel-electrical drive', *Proceedings of the Intersociety Energy Conversion Engineering Conference 23rd*, IEEE Service Center, Piscataway, NJ, pp. 75-80.

Hewko, L.O. and Weber, T.R. 'Hydraulic energy storage based hybrid propulsion system for a terrestrial vehicle', *Proceedings of the Intersociety Energy Conversion Engineering Conference*, IEEE, (IEEE Cat. No. 90CH2942-1), IEEE, Piscataway, NJ Vol. 4, pp. 99-105.

Huhtala, K. (1996) 'Modeling of hydrostatic transmission—steady state, linear and non-linear models', *Acta Polytechnica Scandinavica*, Mechanical Engineering Series, No. 123.

Hung, Y.-H, Lin, P.-H. and Hong, C.-W. (2002) 'A rule-based control algorithm for hybrid electric motorcycle powertrain systems', *Proceedings of the 6th International Symposium on Advanced Vehicle Control*, Hiroshima, Japan.

Jalil, N., Kheir, N.A. and Salman, M. (1997) 'Rule-based energy management strategy for a series hybrid vehicle', *Proceedings of the 1997 American Control Conference*, 19970604-19970606 IEEE, Albuquerque, NM, Part 1 (of 6).

Kang, J., Kolmanovsky, I. and Grizzle, J.W. (2001) 'Dynamic optimization of lean burn engine aftertreatment', *ASME Journal of Dynamic Systems*, *Measurement and Controls*, June, Vol. 123, No. 2, pp. 153-160.

Karnopp, D.C., Margolis, D.L. and Rosenberg, R.C. (1990) *System Dynamics: A Unified Approach*, ISBN 0471-62171-4, Wiley-Interscience, New York, NY.

Kosowski, M.G. and Desai, P.H. (2000) 'A parallel hybrid traction system for General Motors Corporation's 'Precept' PNGV vehicle', SAE paper 2000-01-1534, Warrendale, PA.

Lin C., Filipi Z., Wang Y., Louca L., Peng H., Assanis D. and Stein J. (2001) 'Integrated, feed-forward hybrid electric vehicle simulation in SIMULINK and its use for power management studies', SAE Paper 2001-01-1334, Warrendale, PA.

Lin, C., Kang, J., Grizzle, J. W. and Peng, H. (2001) 'Energy management strategy for a parallel hybrid electric truck', Proceedings of the 2001 American Control Conference, Arlington, VA, June, pp. 2878-2883.

Lin, C., Kang, J., Grizzle, J. W. and Peng, H. (2002) 'Power management strategy for a parallel hybrid electric truck', *Proceedings of the 10th Mediterranean Conference on Control and Automation*, July, Lisbon, Portugal.

Louca, L. S., Rideout G., Stein, J. and Hulbert, G. M. (2003) 'Generating proper models for truck mobility and handling', *International Journal of Heavy Vehicle Systems*.

Louca, L.S. and Yildir, U.B. (2003) 'Modeling and reduction techniques for studies of integrated hybrid vehicle systems', *Proceedings of the 4th International Symposium on Mathematical Modelling*, published in the series ARGESIM-Reports, ISBN 3-901608-24-9, Vienna, Austria.

Lunani M., Sudjianto A. and Johnston P.L. (1995) 'Generating efficient training samples for neural networks using Latin hypercube sampling', *Artificial Neural Networks In Engineering*, November.

Marr, W.W., Sekar, R.R. and Ahlheim, M.C. (1993) 'Analysis of a diesel-electric hybrid urban bus system', SAE paper 931796, Warrendale, PA.

McKay, M.D., Beckman R.J. and Conover W.J. (1979) 'A comparison of three methods for selecting values of input variables in the analysis of output from a computer code', *Technometrics*, May, Vol. 21, No.2.

Moore, T.C. (1996) 'Tools and strategies for hybrid electric drivetrain optimisation', SAE paper 961660, Warrendale, PA.

Pacejka, H.B. and Bakker, E. (1993) 'Tyre models for vehicle dynamics analysis', *Proceedings of the 1st International Colloquium on Tyre Models for Vehicle Dynamics Analysis*, Delft, The Netherlands.

Papalambros P. and Wilde D.J. (2000) *Principles of Optimal Design*, Cambridge University Press, UK.

Pourmovahed, A., Beachley, N.H., and Fronczak, F.J. (1992) 'Modeling of a hydraulic energy regeneration system—part I: analytical treatment', *Journal of Dynamic Systems, Measurement, and Control*, March, Vol. 114, pp. 155-159.

Stein M. (1987) 'Large sample properties of simulations using Latin hypercube sampling', *Technometrics*, May, Vol. 29, No. 2.

Triger, L., Paterson, J. and Drozdz, P. (1993) 'Hybrid vehicle engine size optimization', SAE paper 931793, Warrendale, PA.

Van den Bossche, P. (1999) 'Power sources for hybrid buses: Comparative evaluation of the state of the art', *Journal of Power Sources*, Vol. 80, No. 1, pp. 213-216.

Wilson, W.E. (1946) 'Rotary-pump theory', *Transactions of the ASME*, May, Vol. 67, No. 4, pp. 371-384.

Won, J.-S. and Langari, R. (2002) 'Fuzzy torque distribution control for a parallel hybrid vehicle', *Expert Systems*, February, Vol. 19, No. 1, pp. 4-10.

Wu B., Lin, C.-C., Filipi, Z., Peng, H. and Assanis, D. (2002) 'Optimization of power management strategies for a hydraulic hybrid medium truck', *Proceedings of the 6th International Symposium on Advanced Vehicle Control*, Hiroshima, Japan.

Zhang, G., Filipi, Z.S. and Assanis, D.N. (1997) 'Flexible, reconfigurable, transient multi-cylinder diesel engine simulation for system dynamics studies', *Mech. Struct. Mach*., August, Vol. 25, No. 3, pp. 357-378.

Appendix

Vehicle specifications used during simulation

Diesel engine specifications

Configuration	V6, turbocharged, intercooled
Rated power [kW]	246 @ 2400 rpm
Displacement [l]	7.24
Bore [mm]	110
Stroke [mm]	127
Compression ratio	16:1

Drivetrain specifications

Transmission – 1st gear efficiency	0.9661
Transmission – 2nd gear efficiency	0.9743
Transmission – 3rd gear efficiency	0.9767
Transmission – 4th gear efficiency	0.9788
Transmission – 5th gear efficiency	0.985
Transmission – 6th gear efficiency	0.9772
Transmission – 7th gear efficiency	0.9761

Transmission – 1st gear ratio	6.929
Transmission – 2nd gear ratio	4.1846
Transmission – 3rd gear ratio	2.2371
Transmission – 4th gear ratio	1.6911
Transmission – 5th gear ratio	1.2
Transmission – 6th gear ratio	0.8998
Transmission – 7th gear ratio y	0.783
Propshafts/differential – differential drive ratio	7.8
Propshafts/differential – differential efficiency	0.8944

Vehicle dynamics specifications

CG location from front axle [m]	2.34
Wheelbase [m]	4.1
Rear tandem spacing [m]	1.4
Sprung mass [kg]	11532
Unsprung mass rear1 [kg]	1330.9
Unsprung mass rear2 [kg]	1330.9
Unsprung mass front [kg]	1127.8
Wheel radius [m]	0.572
Aerodynamic drag	0.75
Frontal Area [m^2]	7.43

Baseline hydraulic pump/motor specifications

Maximum displacement [cm3/rev]	150
Fluid bulk modulus of elasticity, β [MPa]	1660
Coefficient of laminar leakage, Cs	3.647×10^{-8}
Coefficient of turbulent leakage, Cst	4.200×10^{-4}
Coefficient of viscous friction, Cv	1227
Coefficient of friction, Cf	0.0384